Reversible Swarming and Separation of Self-Propelled Chemically Powered Nanomotors under Acoustic Fields

8 AUTHORS, INCLUDING:

Fernando Soto
University of California, San Diego
9 PUBLICATIONS   103 CITATIONS

Wei Gao
University of California, Berkeley
59 PUBLICATIONS   1,815 CITATIONS

Renfeng Dong
South China University of Technology
15 PUBLICATIONS   127 CITATIONS

Ernesto Magana
University of California, San Diego
1 PUBLICATION   10 CITATIONS

Reversible Swarming and Separation of Self-Propelled Chemically Powered Nanomotors under Acoustic Fields

Tailin Xu,[†,‡] Fernando Soto,[†] Wei Gao,[†] Renfeng Dong,[†] Victor Garcia-Gradilla,[†] Ernesto Magaña,[†] Xueji Zhang,[‡] and Joseph Wang*[†]

[†]Departments of Nanoengineering, University of California San Diego, La Jolla, California 92093, United States
[‡]Research Center for Bioengineering and Sensing Technology, University of Science and Technology Beijing, Beijing 100083, PR China

S *Supporting Information*

ABSTRACT: The collective behavior of biological systems has inspired efforts toward the controlled assembly of synthetic nanomotors. Here we demonstrate the use of acoustic fields to induce reversible assembly of catalytic nanomotors, controlled swarm movement, and separation of different nanomotors. The swarming mechanism relies on the interaction between individual nanomotors and the acoustic field, which triggers rapid migration and assembly around the nearest pressure node. Such on-demand assembly of catalytic nanomotors is extremely fast and reversible. Controlled movement of the resulting swarm is illustrated by changing the frequency of the acoustic field. Efficient separation of different types of nanomotors, which assemble in distinct swarming regions, is illustrated. The ability of acoustic fields to regulate the collective behavior of catalytic nanomotors holds considerable promise for a wide range of practical applications.

Collective behavior, involving a variety of cooperative arrangements such as aggregation, assembly and migration, is a common phenomenon in the biological world, displayed by many groups of animals, such as ants and bees.[1−3] Such behavior of biological systems has recently inspired the design of synthetic nanomachines that can cooperate with each other or swarm under different external stimuli.[4−7] The ability to regulate the collective behavior of nanomotors outside living systems offers considerable promise for creating groups of machines that can perform cooperative tasks that would be impossible using a single nanomotor. Yet, while major advances have been made in designing powerful self-propelled catalytic micromotors,[8−15] the assembly and cooperation of individual micromotors have reached limited success. For example, Sen, Mallouk and co-workers used light to induce the swarming of inert SiO_2 or AgCl particles[4] and to propel TiO_2 and SiO_2/TiO_2 Janus particles.[5] We described the schooling behavior of gold microparticles triggered by the addition of hydrazine.[6] Solovev et al. reported that self-propelled tubular microengines can organize into more complex entities.[7] Most of the methods used for swarming of synthetic microparticles rely on a self-diffusiophoresis mechanism where an external stimulus generates a concentration gradient that promotes particle migration, and are thus slow and irreversible.[5,6]

Herein we demonstrate for the first time the use of an acoustic field to trigger the assembly of chemically powered nanomotors, including efficient and reversible swarming, controlled movement of the motor assembly and separation of different types of nanomotors. Acoustic fields have been shown previously to be useful for manipulating microparticles due to their noncontact character and compatibility with biological systems.[15−18] However, their utility for creating defined assemblies of catalytic nanomotors has not been reported.

In the present work, we took advantage of such acoustic nanoparticle manipulation for organizing chemically powered autonomously moving motors. Such attractive swarming behavior of chemically powered nanomotors is based on the acoustically generated pressure gradients (generated by a piezoelectric transducer[19−21] as detailed in the Supporting Information (SI)), which results in migration of catalytic nanomotors toward low-pressure regions (nodes or antinodes; Figure 1b,d). Such migration results in the rapid localization
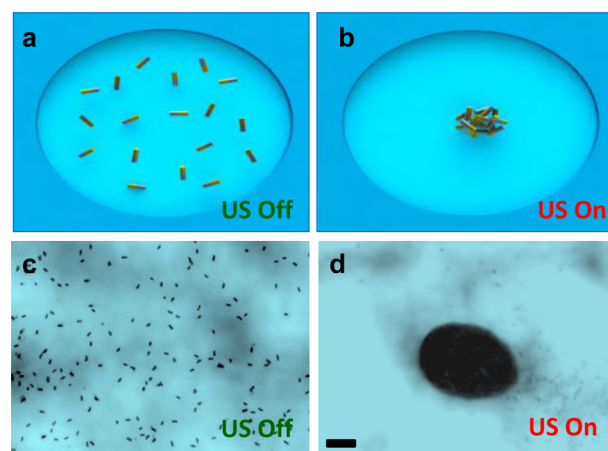

Figure 1. Schematic (a,b) and microscopic images (c,d) illustrating the swarming behavior of chemically powered Au−Pt nanomotors (a,b) under the acoustic radiation forces (b,d). Scale bar, 10 μm; ultrasound field: applied voltage, 10 Vpp, frequency, 618 kHz. Concentration of nanomotors, ~5 × 10³/μL. Image taken from Video S1 (SI).
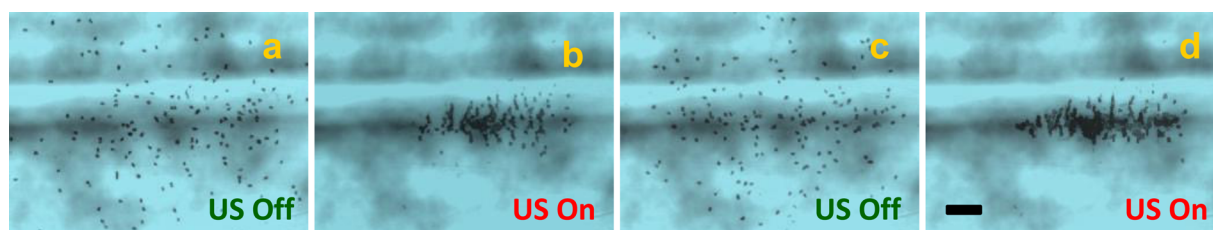
Figure 2. Ultrasound-triggered reversible swarming and dispersion of Pt−Au nanowire motors. (a,c) Catalytic nanomotors swimming autonomously by the decomposition of hydrogen peroxide fuel; image c was obtained 5 s after turning off the acoustic field. (b,d) Rapid ultrasound-triggered assembly of nanomotors into a swarm; images, taken from Video S2 (SI), obtained 2 s after applying the acoustic field. Scale bar, 10 μm; ultrasound conditions as in Figure 1. Concentration of nanomotors, ∼200/μL.

and swarming of nanomotors in these low-pressure regions, as predicted by the acoustic radiation forces theory.[22−24] Unlike ultrasound-based particle manipulation,[22,23] the nanomotor swarms disperse rapidly when the ultrasound field is turned off due to the autonomous catalytic propulsion. Controlled movement of the entire nanomotor assembly is accomplished by regulating variables of the acoustic field (e.g., frequency or voltage), and hence the location of the nodes or antinodes. Compared to previous nanomotor swarming studies, the new swarming process is extremely fast and reversible. Such ability to assemble catalytic nanomotors and regulate their collective behavior offers considerable promise for far-reaching implications in nanomedicine, cargo transport, nanomachinery, and chemical sensing.

The catalytic Pt−Au nanowire motors (diameter: 200 nm, length: 2 μm) used in this study display autonomous motion based on the asymmetric decomposition of hydrogen peroxide that converts chemical energy to mechanical energy.[25] Application of the acoustic field results in the generation of a standing wave, which causes the catalytic nanomotors to migrate toward pressure nodes and rapidly form a swarm, as demonstrated in Figure 1 and corresponding Video S1 (SI). The nanomotors remain assembled as long as the acoustic field is applied since the acoustic force acting on the nanomotors is nearly 8 fold larger than the force resulting from the electrophoretic propulsion (see Supporting Information).[26]

The swarming of the nanomotors is dependent on their interaction with the incident ultrasound mechanical waves.[22,24] Application of the acoustic field results in a planar standing wave, arising from the superposition of two waves with equal amplitudes and wavelengths, but traveling in opposite directions (one wave is generated by the transducer, and the other reflected by the cover slide; Figure S2, SI). The interference between the two waves produces a standing wave that leads to the formation of nodes and antinodes and results in pressure gradients, which drive the nanomotors toward low-pressure regions. The acoustic force can be divided into the primary radiation force (PRF) and the secondary radiation force (SRF). The PRF, which is the main force in the field of acoustic waves, can be subdivided into an axial component (F_z) and a transverse component (F_{xy}), (Figure S1, SI). The F_z component of the PRF is the force that drives the migration of microparticles to the nearest pressure node or antinode plane, while the F_{xy} component leads to their aggregation within the nodal plane.[22] Further aggregation is facilitated by the SRF, which is associated with the sound waves that are scattered by individual nanomotors. The SRF is responsible for particle−particle interactions and makes them either attract or repel each other, as well as forming stable multiparticle spherical structures.[22] Note that there are usually multiple pressure nodes or antinodes in one ultrasound system and the location of the pressure node and antinode can be estimated from the wavelength.[27] However, low frequency used here (kHz level) make the distance between two nodes in our system much larger than field of view of the microscope.

The swarming of the catalytic Au−Pt nanowire motors can be actively reversed, with defined transitions between the dispersed and assembled states through repeated ultrasound stimuli. Such reversible swarming behavior of catalytic nanomotors is demonstrated in Figure 2 and Video S2 (SI). Initially, the catalytic nanowire motors display their typical autonomous motion in the presence of the peroxide fuel and absence of the acoustic field (Figure 2a). Application of the acoustic field leads to rapid migration of the nanowire motors toward the node and formation of an organized structure within 2 s (Figure 2b). Such swarming persists while the acoustic field is applied. Upon removal of the acoustic field, the electrophoretic propulsion dominates and the nanomotor swarm disperses rapidly, with autonomous catalytic motion of the individual nanomotors in the peroxide fuel observed within 5 s (Figure 2c). Such assembled and disassembled nanomotors remain functional after 30 cycles; the process can be repeated until the peroxide fuel is depleted. Such ability to induce a fully reversible swarming, with rapid formation and dispersion of the nanomotors (within few seconds), represents a significant improvement compared to early studies involving the slow swarming of microparticles (Table S1, SI).[4−7,28−32] It should be noted that the motor dispersion and degree of reversibility depends on the motor concentration. At high nanomotor concentrations (e.g., 5000/μL), the secondary radiation force (SRF) is larger due to increased interactions between nanomotors, leading to a more compact spherical structure (e.g., Figure S1, SI).[33] Under these conditions, some of the nanomotors may remain aggregated even after the acoustic field is turned "off", reflecting the larger electrostatic interactions associated with the self-generated electric field on the surface of the Au−Pt nanowires.[34] Decreasing the nanomotor concentration, reduces the motor aggregation (e.g., Figure 2b) and allows for the reversible swarming behavior observed in Figure 2.

The ability to regulate the rate of swarm aggregation and dispersion depends on understanding the parameters that govern these processes. As demonstrated in Figure S3A (SI), it is possible to regulate the swarming speed of the nanomotors by varying the voltage applied to the ultrasound transducer and hence the acoustic power.[19] Faster average swarming speeds (speed of nanomotors migration toward nodes) of 19.5, 40.4, 53.6, 84.8, and 117.4 μm/s are observed upon increasing the applied voltage to 2, 4, 6, 8, and 10 Vpp, respectively. Such dependence reflects the nearly linear relationship between the

PRF and the pressure amplitude. The average velocity of the individual nanomotors remains nearly the same before and after their assembly, indicating negligible effect of the ultrasound radiation on the nanomotors or the hydrogen peroxide fuel. As expected,[25] the speed of Au−Pt nanomotors increases upon increasing peroxide concentration (Figure S3B, SI). Apparently, the larger speed (at higher hydrogen peroxide levels) leads to a faster dispersion of the swarm (upon turning the acoustic field off).[26]

The resulting nanomotor swarm can be moved in a controlled manner by varying the applied acoustic frequency, which changes the ultrasound wavelength. This wavelength shift leads to changes in the location of the pressure nodes and hence in migration of the swarm toward the new location.[27,33] Frequency modulation has been used to manipulate microparticles,[23] but not toward the manipulation of nanomotors or their swarms. Figure 3 and corresponding Video S3 (SI)
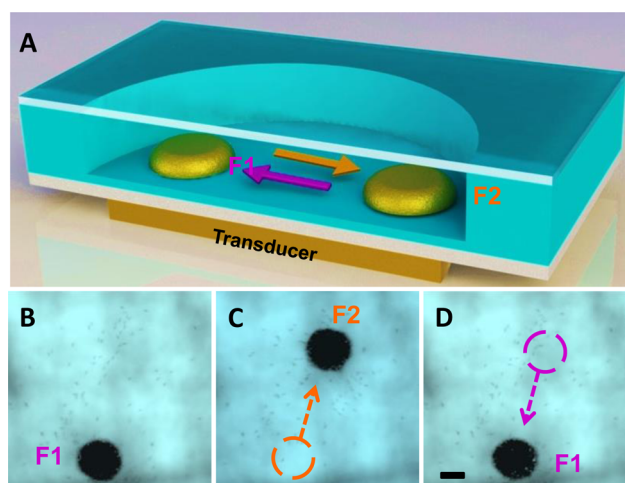

Figure 3. Controlled movement of the organized nanomotor assembly by changing the applied acoustic frequency and hence the location of the low pressure region. (A) Schematic illustration and (B,C,D) actual images, taken from Video S3 (SI), demonstrating the swarm translation upon changing the applied frequency between 628 kHz (F_1) and 618 kHz (F_2) using a transducer power of 10 Vpp. Scale bar, 20 μm. Motor concentration as in Figure 1

illustrate such controlled and reversible movement of the nanomotor swarm between two positions by switching the applied acoustic frequency between 618 kHz (F_1, Figure 3B, D) and 628 kHz (F_2, Figure 3C). As illustrated in the corresponding Video S3 (SI), such change in frequency results in a rapid (∼2 s) movement of the entire swarm over a 90 μm distance. The nanomotor swarm returns rapidly to its original position upon reapplying the original frequency (F_1, Figure 3D). Notice that the nanomotor swarm maintains its compact (spherical) shape during such reversible movement, reflecting the secondary radiation force.[33] Obviously, the use of different frequencies and hence pressure nodes can lead to controlled movement of the motor swarm between multiple locations (Video S3, SI). Such ability to switch the swarm location is important for practical applications in nanomedicine or cargo transport. For example, moving the swarm to a target region and allowing it to disperse by self-propulsion to treat specific objects in its vicinity.

To expand the practical utility of the reversible swarming behavior of nanomotors we evaluated and demonstrated the

capability of separating different types of catalytic nanomotors under ultrasound excitation. Acoustic separation of two populations of particles has been reported, but not in connection to moving nanomotors.[35] Such capability was illustrated for the separation of Au−Pt nanowires and spherical Pt-polymer Janus microparticles (diameter: 1.21 μm) (Figure 4
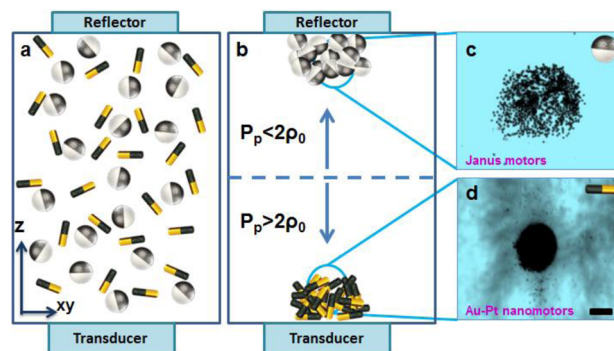

Figure 4. Ultrasound triggered separation of different types of catalytic nanomotors. (a) Schematic of the spherical Janus motors and Au−Pt nanowires motors in the ultrasound set up. Schematic (b) and actual images (c,d) of the acoustic-induced swarming and separation of Janus microsphere motors (c) and catalytic Au−Pt nanowire motors (d) taken from Video S4 (SI). Ultrasound conditions as in Figure 1.

and Video S4, SI). These nanomotors were selected due to their different material properties (detailed in Table S2, SI). Initially, without the acoustic field, both of these catalytic nanomotors display autonomous movement in the presence of hydrogen peroxide fuel (a). Upon application of the acoustic field, the Au−Pt nanowires form a swarm near the bottom of the cell (d) while the Janus microparticles migrate and assemble near the cover glass slide (c).

The separation of different types of particles under acoustic field represents an important challenge.[22] Doinikov's theory indicates that if the radius of the sphere (R_0) is significantly smaller than the penetration depth of the viscous (δ_v) and thermal (δ_t) wave in the host fluid, it is possible to separate different kinds of particles by a radiation force (F) in a plane standing wave.[33]

$$F = \pi\rho_0 |A|^2 \sin(2kd)(kR_0)^3\left[\frac{2\rho_0 - \rho_p}{3\rho_0} + O\left(\frac{R_0}{\delta_v}, \frac{R_0}{\delta_t}\right)\right]$$

(1)

where ρ_0 is the fluid density at rest, A is the complex amplitude of the velocity potential of the imposed sound field, d is the distance between the equilibrium center of the sphere and the nearest velocity node plane of the standing sound wave, $k = \omega/c$ is the wavenumber in the fluid, c is the speed of sound in the fluid, R_0 is the radius of the sphere (note that, by assumption, $kR_0 = 0.00025 \ll 1$, the effect of elasticity is negligible). Doinikov's theory has provided insights as to why particles disperse due to a density difference. The density of the Au−Pt nanowire motors ($\rho_p = 20.5$ g/cm^3) is much larger than that of the medium ($\rho_0 = 0.997$ g/cm^3); therefore, the radiation force ($F < 0$) makes these nanomotors migrate toward the pressure antinodes located at the bottom of the cell. In contrast, the density of Janus nanomotors is significantly smaller than $2\rho_0$ ($\rho_p = 1.1$ g/cm$^3 < 2\rho_0$); hence, the radiation force ($F > 0$) drives the microsphere motors to be driven toward pressure nodes located at the top of the cell. Particles with different sizes

are expected to display different swarming speeds toward the pressure node or antinode, with smaller particles moving slower.[36] However, particles with same density would swarm to the same place independent of their shape and size. The ability to impart different swarming locations on catalytic nanomotors, depending on their specific properties, offers a new approach for on-demand isolation, extraction or concentration of nanomotors for a wide range of applications in fields such as nanomedicine nanofabrication, or cargo transport.

In conclusion, we have demonstrated the ability of acoustic fields to trigger the assembly of chemically powered nanomotors and to regulate the collective behavior of such catalytic motors. In particular, attractive new capabilities have been illustrated, including the rapid and reversible swarm formation, controlled movement of the entire motor assembly and separation of different types of chemically powered nanomotors. The observed behavior has been attributed to the formation of acoustically generated pressure gradients, which lead to the rapid migration and assembly of the catalytic nanomotors around the nearest low-pressure region. This ability of acoustic fields to regulate the collective behavior of catalytic nanomotors indicates considerable promise for creating man-made nanomachines that function collectively and mimic the swarming of animals. These attractive capabilities and new observations offer considerable promise for a wide range of practical applications ranging from chemical sensing to nanomachinery and drug delivery.

■ ASSOCIATED CONTENT

Ⓢ Supporting Information

Experimental section, additional figures, tables and videos. This material is available free of charge via the Internet at http://pubs.acs.org.

■ AUTHOR INFORMATION

Corresponding Author

josephwang@ucsd.edu

Notes

The authors declare no competing financial interest.

■ ACKNOWLEDGMENTS

■ REFERENCES

(1) Sumpter, D. *Philos. Trans. R. Soc., B* **2006**, *361*, 5.
(2) Poli, R.; Kennedy, J.; Blackwell, T. *Swarm Intell.* **2007**, *1*, 33.
(3) Vicsek, T.; Zafeiris, A. *Phys. Rep.* **2012**, *517*, 71.
(4) Ibele, M.; Mallouk, T. E.; Sen, A. *Angew. Chem., Int. Ed.* **2009**, *48*, 3308.
(5) Hong, Y.; Diaz, M.; Cordova-Figueroa, U. M.; Sen, A. *Adv. Funct. Mater.* **2010**, *20*, 1568.
(6) Kagan, D.; Balasubramanian, S.; Wang, J. *Angew. Chem., Int. Ed.* **2011**, *50*, 503.
(7) Solovev, A. A.; Sanchez, S.; Schmidt, O. G. *Nanoscale* **2013**, *5*, 1284.
(8) Wang, J. *Nanomachines: Fundamentals and Applications*; John Wiley & Sons: New York, 2013.
(9) Wang, J.; Gao, W. *ACS Nano* **2012**, *6*, 5745.
(10) Wang, W.; Duan, W.; Ahmed, S.; Mallouk, T. E.; Sen, A. *Nano Today* **2013**, *8*, 531.
(11) Guix, M.; Mayorga-Martinez, C. C.; Merkoci, A. *Chem. Rev.* **2014**, *114*, 6285.
(12) Gao, W.; Wang, J. *ACS Nano* **2014**, *8*, 3170.
(13) Sanchez, S.; Pumera, M. *Chem.—Asian J.* **2009**, *4*, 1402.
(14) Mei, Y.; Solovev, A. A.; Sanchez, S.; Schmidt, O. G. *Chem. Soc. Rev.* **2011**, *40*, 2109.
(15) Sengupta, S.; Ibele, M. E.; Sen, A. *Angew. Chem., Int. Ed.* **2012**, *51*, 8434.
(16) Shi, J.; Ahmed, D.; Mao, X.; Lin, S. C.; Lawit, A.; Huang, T. J. *Lab Chip* **2009**, *9*, 2890.
(17) Vanherberghen, B.; Manneberg, O.; Christakou, A.; Frisk, T.; Ohlin, M.; Hertz, H. M.; Onfelt, B.; Wiklund, M. *Lab Chip* **2010**, *10*, 2727.
(18) Raeymaekers, B.; Pantea, C.; Sinha, D. N. *J. Appl. Phys.* **2011**, *109*, 014317.
(19) Xu, T.; Soto, F.; Gao, W.; Garcia-Gradilla, V.; Li, J.; Zhang, X.; Wang, J. *J. Am. Chem. Soc.* **2014**, *136*, 8552.
(20) Wang, W.; Castro, L. A.; Hoyos, M.; Mallouk, T. E. *ACS Nano* **2012**, *6*, 6122.
(21) Garcia-Gradilla, V.; Orozco, J.; Sattayasamitsathit, S.; Soto, F.; Kuralay, F.; Pourazary, A.; Katzenberg, A.; Gao, W.; Shen, Y.; Wang, J. *ACS Nano* **2013**, *7*, 9232.
(22) Woodside, S. M.; Bowen, B. D.; Piret, J. M. *AIChE J.* **1997**, *43*, 1727.
(23) Tran, S. B. Q.; Marmottant, P.; Thibault, P. *Appl. Phys. Lett.* **2012**, *101*, 114103.
(24) Laurell, T.; Petersson, F.; Nilsson, A. *Chem. Soc. Rev.* **2007**, *36*, 492.
(25) Paxton, W. F.; Sen, A.; Mallouk, T. E. *Chem.—Eur. J.* **2005**, *11*, 6462.
(26) Happel, J.; Brenner, H. *Low Reynolds Number Hydrodynamics*; Springer: Amsterdam, 1983.
(27) Ding, X.; Lin, S. C.; Kiraly, B.; Yue, H.; Li, S.; Chiang, I. K.; Shi, J.; Benkovic, S. J.; Huang, T. J. *Proc. Natl. Acad. Sci. U. S. A.* **2012**, *109*, 11105.
(28) Duan, W.; Liu, R.; Sen, A. *J. Am. Chem. Soc.* **2013**, *135*, 1280.
(29) Hernàndez-Navarro, S.; Tierno, P.; Farrera, J. A.; Ignés-Mullol, J.; Sagués, F. *Angew. Chem., Int. Ed.* **2014**, *126*, 10872.
(30) Solovev, A. A.; Mei, Y.; Schmidt, O. G. *Adv. Mater.* **2010**, *22*, 4340.
(31) Ibele, M. E.; Lammert, P. E.; Crespi, V. H.; Sen, A. *ACS Nano* **2010**, *4*, 4845.
(32) Gao, W.; Pei, A.; Dong, R.; Wang, J. *J. Am. Chem. Soc.* **2014**, *136*, 2276.
(33) Doinikov, A. A. *Recent Res. Devel. Acoust.* **2003**, *1*, 39.
(34) Wang, W.; Duan, W.; Sen, A.; Mallouk, T. E. *Proc. Natl. Acad. Sci. U. S. A.* **2013**, *110*, 17744.
(35) Zhang, J.; Meng, L.; Cai, F. Y.; Zheng, H. R.; Courtney, C. R. P. *Appl. Phys. Lett.* **2014**, *104*, 224103.
(36) Ding, X.; Peng, Z.; Lin, S. C.; Geri, M.; Li, S.; Li, P.; Chen, Y.; Dao, M.; Suresh, S.; Huang, T. J. *Proc. Natl. Acad. Sci. U. S. A.* **2014**, *111*, 12992.